

# Inhibition of Amyloid Fiber Formation by Peptide-Based Inhibitors

Author: Katherine Gleason

Persistent link: <http://hdl.handle.net/2345/535>

This work is posted on [eScholarship@BC](#),  
Boston College University Libraries.

---

Boston College Electronic Thesis or Dissertation, 2008

Copyright is held by the author, with all rights reserved, unless otherwise noted.

Boston College

College of Arts and Sciences Honors Program

Biology Department

“Inhibition of Amyloid Fiber Formation by Peptide-  
Based Inhibitors”

Katherine Gleason

April 29, 2008

Advisor: Dr. Daniel Kirschner

## **Abstract**

Alzheimer's disease is the leading cause of dementia in the United States. The neurodegenerative condition of this disease correlates with the formation in the brain of plaques consisting of insoluble protein aggregates, termed amyloid. The aggregates are caused by the misfolding of amyloid  $\beta$ , a 40–42 amino acid polypeptide that is naturally occurring in all humans. One approach to preventing the amyloid cytotoxicity is to prevent the formation of plaques altogether. Many types of inhibitors have been tested for their therapeutic value, including substituted peptide strands. In this study, the inhibitory potential of two such peptides was tested: methylated peptides and nitrile-substituted peptides. A $\beta$ (16-22) was used for its fiber-forming properties, and x-ray diffraction and transmission electron microscopy were used to assess the extent of fibrillogenesis. The methylated peptide effectively inhibited fiber formation as previously recorded, and the cyanophenylalanine derivatives did not form fibers. The latter experiment provided insight on the structural and folding properties of A $\beta$  more than its possible inhibitory potential.

**Key words:** protein, amyloid, methylation, cyanophenylalanine, x-ray diffraction, electron microscopy

## Table of Contents

1. Introduction.....	3
2. Methods.....	8
3. Results.....	10
4. Discussion.....	12
5. Conclusion.....	15
6. References.....	16
7. Figures.....	18



## Introduction

Alzheimer's Disease is a neurodegenerative disease that affects millions of people every year. One of the causative agents of AD is the fibrillogenesis of  $\beta$ -amyloid, a 42-strand protein cleaved from amyloid precursor protein (1). Research for AD prevention or for therapeutics normally stem from: inhibition of  $A\beta$  expression or fibrillogenesis, inhibition of the proteases that cleave  $A\beta$  from APP, and alleviating disease symptoms by methods unrelated to amyloidosis, such as trying to re-grow killed cells or enhance the remaining cells (2). Since APP is a naturally occurring protein, and the secretases that cleave it to form  $A\beta$  are proven to have other biologically significant roles, the inhibition of the secretases is not a viable option, nor is preventing expression of  $A\beta$  (3). Though medications that enhance synaptic efficiency are now the only therapeutic avenue available to those with AD, their efficacy is limited. All treatments that minister to the symptoms but not the etiological pathway will run into this hurdle since the neurons will continue to die in the presence of the cytotoxic protein species. Also, research in such uniquely  $A\beta$  pathways and effects can not directly provide information about other amyloid diseases. Since it is likely that any polypeptide chain can aggregate into insoluble fibrils, and amyloid disease affect several different parts of the body, an avenue that can apply to inhibition of fibrillogenesis, as opposed to only  $A\beta$ , would be beneficial. (4). Therefore, the principal research for AD therapeutics should be the prevention or control of  $A\beta$  fibrillogenesis and its toxic form (3).

There has been much debate over which form of the  $A\beta$  peptide is responsible for neuronal death. The "amyloid hypothesis" originally assumed that the insoluble fiber was the guilty agent. The fiber exhibits characteristic Congo Red binding properties, a trait

manipulated in many early amyloid experiments. Since the presence of fibers was confirmed in this way in the autopsied brains of those with AD, it was hypothesized that they caused the cell death. Later studies showed that the oligomeric form of the peptide is in equilibrium with the fibers (4), something not seen because the oligomer does not exhibit green birefringence when stained with Congo Red like the fiber. Recently the toxic effect of the oligomeric form has been shown in vitro in cell culture. This evidence does not mean the insoluble fiber is necessarily innocuous, and in the case of therapeutics it would be beneficial to consider them both dangerous. Uncertainty as to which form is toxic presents concerns for those seeking to prevent A $\beta$  fibrillogenesis. Driving the oligomeric form to stabilize may cause harmful fibers to form, and disassembling the formed fiber may cause harmful oligomers to form. Also, in an extreme case, the fibers may temper the effects of the toxic oligomers by sequestering them and shielding healthy neurons. The goal, therefore, must be to prevent misfolding and induce the native structure, or to form stable, innocuous monomers or dimers that can be broken down by the body (5). How to reach this goal takes knowledge of the folding properties of A $\beta$ .

Though the pathway is unclear, the structure of the formed amyloid fiber has been studied for over twenty years. Hydrogen bonds bring amino acid strands together to form sheets, the side chains of which then interact to form the fiber. All fibers share a cross- $\beta$  sheet pattern (6), the peptide chains running perpendicular to the long axis of the fiber and the hydrogen bonding running parallel. This creates a fiber of indefinite length (7). Fibril formation begins with the slow formation of a nucleus, which then quickly propagates (8). The driving force of aggregation is unknown, but studies show that hydrophobic interactions are very influential in folding, with electrostatic interactions

playing a lesser role (8, 9). There are two main hydrophobic cores: A $\beta$ (16-22) and A $\beta$ (34-42). The disruption of either of these sections prevents fiber formation, but A $\beta$ (16-22) is the more effective (10) and is assumed to be more important in crystallite formation (11). Its importance in fiber formation and its short sequence makes it an excellent model for inhibition studies, and for creating a peptide-based inhibitor. It stabilizes through rearrangement in the same way A $\beta$ (1-40) is assumed to stabilize, meaning the mechanisms for aggregation of the short peptide can be used to study and understand the mechanisms of the full-length peptide (12).

There are many different classes of potential fibrillogenesis inhibitors, but one of the most rational is peptide-based inhibitors. While other inhibitors can be found through educated guesses and chance, peptides can be specifically designed and manipulated. In most cases, the peptide used is a short segment from the target amyloidogenic protein. This overcomes the problem many small molecules have of affinity, since proteins can in general bind to themselves. Several forms of inhibitors have been synthesized, including peptides with: amino acid substitutions; insertions of D-amino acids; and modification of their backbones, termini, amino acid side chains, and bonds (13). Proline substitutions were very common since they alter secondary structure, entering a characteristic 'kink' in the amino acid folding, but have since been proven ineffective as inhibitors. The 'kink' that may have been beneficial prevented the inhibitor from binding to the wild type strand. D-amino acids were shown to make more effective inhibitors than L-amino acids, even on L-amino acid targets. (5)

Modification of peptide backbones is prevalent in the form of N-methylated peptides. In these strands bulky methyl groups replace hydrogens on the nitrogen in the

peptide backbone. Where the methylations are located affects the efficacy of the inhibitor. David Gordon et al. (2001) showed that alternating methylations on A $\beta$ (16-22) creates a strong inhibitor and disassembler of amyloid fibers. Kokkoni et al (2006) found that a methyl group on any one amino acid in a peptide sequence inhibits fibrillogenesis. The theory behind N-methylated peptides is that the addition of one methyl group or more on one face of the peptide strand forms a two-sided peptide: one that can H-bond with the target protein and one that cannot. This prevents propagation and stifles fiber growth (5). Another method of inhibition could be steric hindrance. For fiber disassembly, it is postulated that the inhibitor binds to the fiber and removes one amino acid strand at a time in a more stable conformation, which can then be broken down (14). This would explain why such a high ratio of inhibitor to amyloid is needed.

Another interesting peptide-based inhibitor is cyanophenylalanine, which involves the addition of a nitrile group to phenylalanine. Experimental use of cyanophenylalanine is becoming more widespread because it is a useful probe for IR and fluorescence experiments (15). Because of the hydrophobicity of phenylalanine, it often is present in the hydrophobic core of enzymes and other proteins, making it a valuable amino acid to follow in the folding process. In A $\beta$ (16-22), there are two phenylalanines: residues 19 and 20. By switching which one contains the nitrile group, the individual significance of each amino acid in the fibrillogenesis pathway can be assayed.

When testing for the efficacy of these two forms of fibrillogenesis inhibitors, it is advisable to use more than one assay since each assay provides insight into different aspects of the protein and its folding (5). One valuable pair is x-ray diffraction (XRD) and electron microscopy (EM) (16). The diffraction pattern of an amyloid fiber is a

characteristic cross- $\beta$  sheet with the hydrogen- bonding direction is reliably around 4.7 Å, and the intersheet stacking direction around 10.0 Å (11). Small changes in both hydrogen bonding and intersheet stacking, therefore, can be detected through x-ray, and the direction of fiber inhibition can be discerned. EM gives visual, morphological support of what was deduced from XRD. These two methods are the most reliable when used in tandem since the structure of A $\beta$  fibrils does not appear to be determined solely by its amino acid sequence or thermodynamics (17) and therefore cannot be deduced by computer or other means that rely on these mechanisms.

## Methods

*Peptides* Peptides were received from the lab of Dr. Sean Decatur of Mount Holyoke College. They were synthesized, purified by HPLC, and then lyophilized. They were then dissolved in 0.05M DCl for six hours for H/D exchange, and lyophilized again. This was then dissolved in 1 mM phosphate buffer at pH 7 at a concentration of 10 mg/mL. The individual peptides were then mixed at the appropriate molar ratio. The samples were: A $\beta$ 16-22, A $\beta$ 16-22 methylated (m), 1:1 molar ratio wild type to inhibitor, and 1:5 molar ratio wild type to inhibitor. The second batch of samples was A $\beta$ (16-22) with a nitrile substitution on: residue 19, residue 20, or both 19 and 20.

*X-ray Diffraction* The peptide solution was aspirated into a 0.7 mm siliconized glass capillary tube (Charles A. Supper, Co., South Natick, MA, USA) to a column height of approximately 10.0 mm. The narrow end was flame sealed and the wide end sealed with wax then punctured with a hot needle to allow for evaporation. They were then allowed to dry down vertically at room temperature in a magnetic field until only a uniform disk remained.

The dried sample was taken to the lab of Dr. Andrew Bohm of the Department of Biochemistry at Tufts University. Measurements were taken using the Oxford Diffraction Xcalibur PX Ultra. The sample was placed 85 mm from the detector, and was exposed to x-rays for 150 seconds. The resulting patterns were translated and background subtracted using CrysAlis RED software. FIT2D and Peak Fit were then used to create an intensity profile, the results of which were then used to determine coherent domain size and lattice spacing using Bragg's Law.

*Transmission Electron Microscopy* Sample solutions were diluted to 0.5 mg/mL and spotted onto a UV- radiated carbon- coated mesh grid for 15 minutes and blotted. Once dried, 2% uranyl acetate was placed on the grids for 15 minutes to negatively stain them. The grids were blotted and allowed to air dry before searching for fiber formation. A Philips CM70 Transmission Electron Microscope at 39,000; 28,500; and 11,500 times magnification was used. Pictures were taken on Kodak film.

## Results

The XRD patterns in Figures 1 and 4 are background subtracted with an empty capillary tube. While there are other bands of high electron density, only those corresponding to hydrogen bonding and intersheet stacking are analyzed. In Figures 2, 5, 6, and 7, the D-spacing refers to the distance between strands or polypeptide sheets (for hydrogen bonding and intersheet stacking respectively). The coherent length is the amount of interactions present, and serves to quantitate the degree of fibrillogenesis. The lyophilized samples serve as a baseline for comparison. The error bars in Figure 7 represent the standard deviations of the samples.

*Methylation Study* The XRD patterns from the four samples show a decrease in the amount of amyloid fiber present dependent on the amount of methylated peptide (Figure 1). As the amount of inhibitor increases, the bands broaden, particularly the intersheet stacking band. While the 1:1 samples are similar to the wild type in the degree of intersheet stacking present, the 1:5 ratio samples are significantly lower. Both also show a greater distance between sheets caused by side chain interactions. In the hydrogen-bonding direction the 1:1 sample has less bonding than the 1:5 sample, but neither is significantly different from the wild type (Figures 2, 7). Not enough data could be collected from the A $\beta$ (16-22)m XRD sample to be analyzed.

In Figure 3, A $\beta$ (16-22) forms fibers morphologically similar to the full-length peptide (3: A). They have diameters of approximately 250 Å, and lengths around 15,000 Å. The presence of A $\beta$ (16-22)m in equal concentration to the wild type alters its conformation, causing it to form wide, flat, plate-like fibers (Figure 3: B-D). These fibers have widths of approximately 1,600 Å and varying lengths from 8,000 Å to 45,000 Å.



*Cyanophenylalanine Study* The weakening of peptide interactions is again obvious from the XRD patterns (Figure 4), especially in the case of F20CN and F19/20CN. In the intersheet stacking direction F19CN shows more stacking than the wild type, and F20CN shows significantly less. Both have an increase between sheets, but F20CN is more pronounced. In the hydrogen bonding direction only the F20CN has a significantly lower coherent length. (Figure 5)

## Discussion

Alzheimer's Disease is devastating, and the formation of inhibitors to A $\beta$  fiber formation is an important step in the development of therapeutics. Peptide-based inhibitors have many valuable qualities and are able to provide insight into the mechanism and structure of fibrillogenesis and amyloid fibers. The hydrophobic core region A $\beta$ (16-22) is a popular peptide for inhibition studies because it is the shortest fiber-forming A $\beta$  segment and is key in the formation of fibers in the full-length 1-40 peptide (14).

The methylation study confirms previous evidence that A $\beta$ (16-22)m inhibits fiber formation. (18) There may have been a problem in the experimental procedure though. The sample preparation was not conducive to XRD experimentation. The dissolving of the wild type peptide and the inhibitor separately, and then combining them, allows the wild type to form fibers in the absence of inhibitor. The decrease in the degree of fibrillogenesis observed may then be the product of decreased A $\beta$ (16-22) concentration as opposed to the interference of the methylated A $\beta$ .

The results differ from previous viewpoints in the formation of structure by A $\beta$ (16-22)m. It has been hypothesized that the methylated peptide does not bind to itself and cannot form fibers on its own (13, 14). From the XRD pattern (Figure 1:D) there is evidence of slight secondary structure. Surprisingly, the darker band of the methylated peptide pattern is the hydrogen- bonding band. Hydrogen bonding is what has been predicted to be the most affected by methylation since they replace the open hydrogen atom with a methyl group. This may be explained by the presence of dimers, formed from hydrogen bonding between the faces of the peptide that are un-methylated. Also,

many researchers explain the process of inhibition as being mainly the product of hydrogen bonding interference, but there is no significant difference in the amount of hydrogen bonding in any sample from the methylation study, only in the amount of intersheet stacking.

The electron micrographs in Figure 3 provide morphological details to the structure of the peptide in the presence of inhibitor. Picture A is similar to previously published micrographs of A $\beta$ (16-22) (19). Pictures B-D show the uniform, high density plate-like fibers formed from equal amounts of wild type A $\beta$ (16-22) and inhibitor which have not been studied before. Their plate appearance is in accordance with the diffraction data. There was comparable hydrogen bonding in the wild type and inhibited samples, so flat fibers could still form. There was decreased intersheet stacking though, and therefore the hydrogen-bonded sheets did not interact and did not form fibrils like the unmethylated sample.

Since the cyanophenylalanine peptides were not tested with the wild type peptides, no insight was gained into their viability as a potential inhibitor. Instead, valuable structural information was revealed, including how the hydrophobic core functions in amyloid folding. This experiment presented further evidence that hydrophobic interactions are paramount in importance for fiber formation, and elucidated the vital role of F20 in such interactions. The addition of a cyanonitrile group to residue 19 did not significantly decrease the amount of secondary structure; in fact it increased the amount of intersheet stacking, though the side-chain interactions resulted in greater spacing between  $\beta$ -sheets. The addition of a cyanonitrile group on the 20<sup>th</sup> residue, though, greatly decreased the amount of fiber formation. The wild type A $\beta$ (16-22)

became ordered during the drying down phase when the peptide strands are able to rearrange to form their most stable conformation. In comparison to the lyophilized F20CN sample, the amount of secondary structure decreased with solubilization and drying. Given the time and space, these strands appear to repel each other and are unable to form any organized structure. These results correspond with the previous findings that A $\beta$ (1-42) with an amino acid substitution on F20 decreases fibril formation and neurotoxicity. (20)

## Conclusion

Methylated A $\beta$ (16-22) does impact the extent of A $\beta$ (16-22) fibrillogenesis. Though the coherent domain size in the hydrogen bonding direction does not vary greatly as the ratio of inhibitor to peptide increases, the domain size of the intersheet stacking decreases. This is supported by TEM and the plate-like fibers seen.

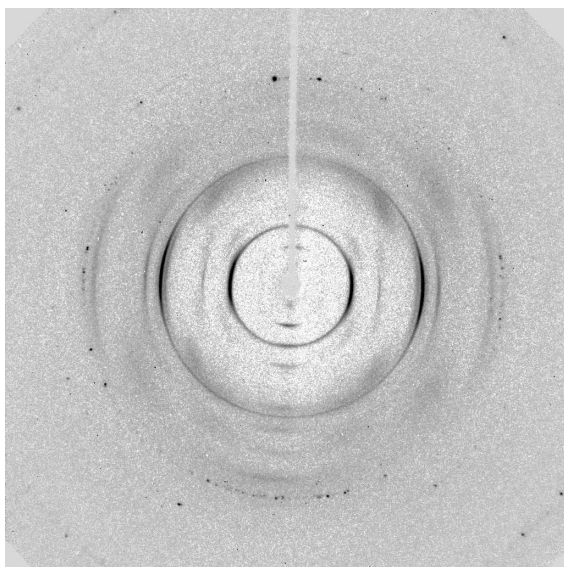
Hydrophobic interactions play significant role in  $\beta$  sheet formation, and F20 is a vital part of this interaction. While a cyanonitrile substitution on phenylalanine 19 is also detrimental to fiber formation, one on 20 almost completely eliminates them. Substituting both phenylalanines denies all secondary structure.

Further research should be done to assess the importance of F20 in longer peptide strains. It is unsurprising that it is influential in A $\beta$ (16-22) since it is only a seven-residue fragment and makes up one hydrophobic core. Its efficacy of fiber prevention should be assessed using a peptide with more amino acids on either side of the core, such as A $\beta$ (10-35), and also on a peptide that encompasses both hydrophobic cores. Also, it should be tested as an inhibitor, mixed with a solution of wild-type A $\beta$ (16-22) and the corresponding longer fragments.

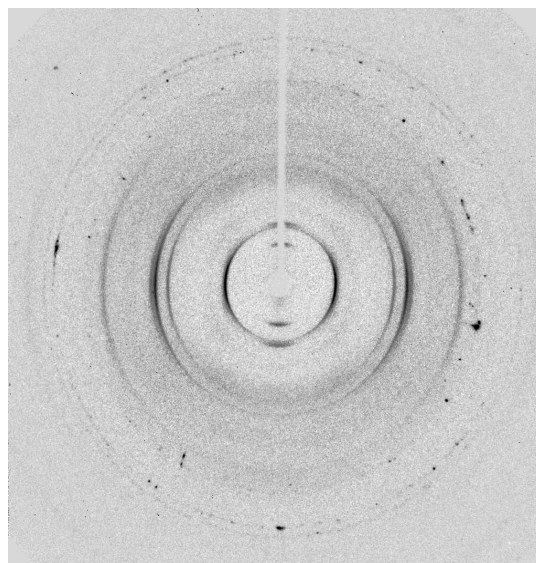
## References

1. Hardy, J., & Selkoe, D. J. (2002) The amyloid hypothesis of Alzheimer's disease: progress and problems on the road to therapeutics, *Science* 297, 353-356.
2. Mason, J. M., Kokkoni, N., Stott, K., & Doig, A. J. (2003) Design strategies for anti-amyloid agents, *Current Opinion in Structural Biology* 13, 1-7.
3. Kokkoni, N., Stott, K., Amijee, H., Mason, J. M., & Doig, A. J. (2006) N-methylated peptide inhibitors of  $\beta$ -amyloid aggregation and toxicity. Optimization of the inhibitor structure, *Biochemistry* 45, 9906-9918.
4. Selkoe, D. J. (2003) Folding proteins in fatal ways, *Nature* 426, 900-904.
5. Sciarretta, K. L., Gordon, D. J., & Meredith, S. C. (2006) Peptide-based inhibitors of amyloid assembly, *Methods in Enzymology* 413, 273-312.
6. Kirschner, D. A., Abraham, C., & Selkoe, D. J. (1986) X-ray diffraction from intraneuronal paired helical filaments and extraneuronal amyloid fibers in Alzheimer disease indicates cross- $\beta$  conformation, *Proc. Natl. Acad. Sci USA* 83, 503-507.
7. Lomakin, A., Teplow, D. B., Kirschner, D. A., & Beneder, G. B. (1997) Kinetic theory of fibrillogenesis of amyloid  $\beta$ -protein, *Proc. Natl. Acad. Sci. USA* 94, 7942-7947.
8. Röhrig, U. F., Laio, A., Tantalo, N., Parrinello, M., & Petronzio, R. (2006) Stability and structure of oligomers of the Alzheimer peptide A $\beta$ (16-22): from the dimer to the 32-mer, *Biophysical Journal* 91, 3217-3229.
9. Balbach, J. J., Ishii, Y., Antzutkin, O. N., Leapman, R. D., Rizzo, N. W., Dyda, F., Reed, J., & Tycko, R. (2000) Amyloid fibril formation by A $\beta$ (16-22), a seven-residue fragment of the Alzheimer's  $\beta$ -amyloid peptide, and structural characterization by solid state NMR, *Biochemistry* 39, 13748-13759.
10. Sciarretta, K. L., Boire, A., Gordon, D. J., & Meredith, S. J. (2006) Spatial separation of  $\beta$ -sheet domains of  $\beta$ -amyloid: disruption of each  $\beta$ -sheet by N-methyl amino acids, *Biochemistry* 45, 9485-9495.
11. Inouye, H., Fraser, P.E., & Kirschner, D. A. (1993) Structure of  $\beta$ -crystallite assemblies formed by Alzheimer  $\beta$ -amyloid protein analogues: analysis by x-ray diffraction, *Biophysical Journal* 64, 502-519.
12. Petty, S.A., & Decatur, S.M. (2005) Experimental evidence for the reorganization of  $\beta$ -strands within aggregates of the A $\beta$ (16-22) peptide, *J. Am. Chem. Soc.* 127, 13488-13489.

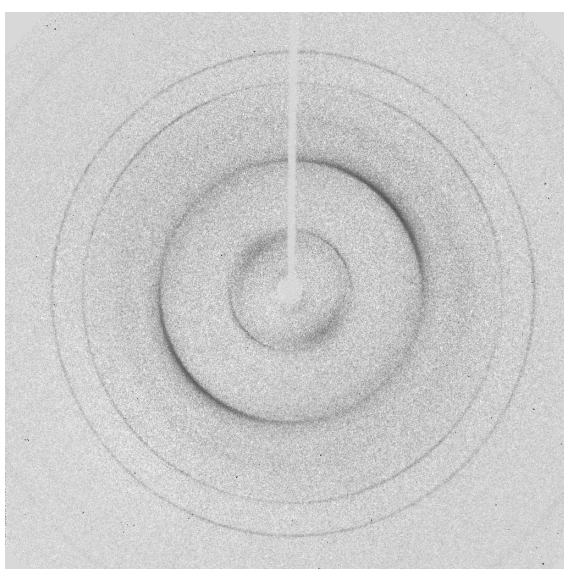
13. Gordon, D. J., & Meredith, S. C. (2003) Probing the role of the backbone hydrogen bonding in  $\beta$ -amyloid fibrils with inhibitor peptides containing ester bonds at alternate positions, *Biochemistry* 42, 475-485.
14. Soto, P., Griffin, M. A., & Shea, J. (2007) New insights into the mechanism of Alzheimer amyloid- $\beta$  fibrillogenesis inhibition by N-methylated peptides, *Biophysical Journal* 93, 3015-3025.
15. Aprilakis, K. N., Taskent, H., & Raleigh, D. P. (2007) Use of novel fluorescent amino acid p-cyanophenylalanine offers a direct probe of hydrophobic core formation during the folding of the N-terminal domain of the ribosomal protein L9 and provides evidence for two-state folding, *Biochemistry* 46, 12308-12313.
16. Malinchik, S. B., Inouye, H., Szumowski, K. E., & Kirschner, D. A. (1998) Structural analysis of Alzheimer's  $\beta$ (1-40) amyloid: protofilament assembly of tubular fibrils, *Biophysical Journal* 74, 537-545.
17. Petkova, A. T., Leapman, R. D., Guo, Z., Yau, W., Mattson, M. P., & Tycko, R. (2005) Self-propagating, molecular-level polymorphism in Alzheimer's  $\beta$ -amyloid fibrils, *Science* 307, 262-265.
18. Gordon, D. J., Sciarretta, K. L., & Meredith, S. C. (2001) Inhibition of  $\beta$ -amyloid(40) fibrillogenesis and disassembly of the  $\beta$ -amyloid(40) fibrils by short  $\beta$ -amyloid congeners containing N-methyl amino acids at alternate residues, *Biochemistry* 40, 8237-8245.
19. Gordon, D. J., Balbach, J. J., Tycko, R., & Meredith, S. C. (2004) Increasing the amphiphilicity of an amyloidogenic peptide changes the  $\beta$ -sheet structure in the fibrils from antiparallel to parallel, *Biophysical Journal* 86, 428-434.
20. Boyd-Kimball, D., Abdul, H. M., Reed, T., Sultana, R., & Butterfield, D. A. (2004) Role of phenylalanine 20 in Alzheimer's amyloid  $\beta$ -peptide (1-42)-induced oxidative stress and neurotoxicity, *Chem. Res. Toxicol.* 17, 1743-1749.



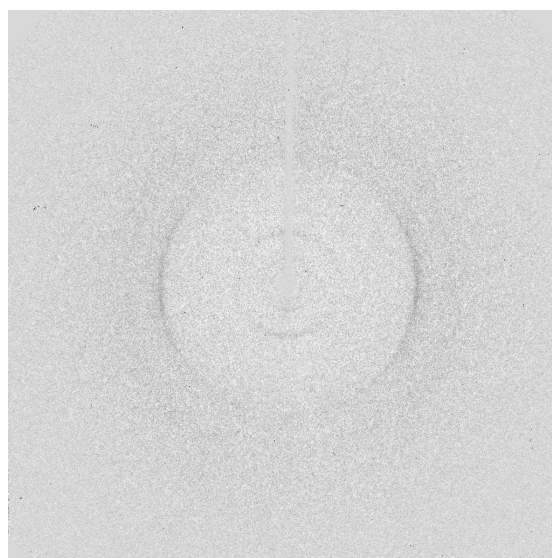
**A.** A $\beta$ (16-22)



**B.** A $\beta$ (16-22): A $\beta$ (16-22)m 1:1



**C.** A $\beta$ (16-22): A $\beta$ (16-22)m 1:5



**D.** A $\beta$ (16-22)m

**Figure 1:** Background-subtracted XRD patterns of solubilized/ dried peptides for the methylation study. A decrease in the sharpness and darkness of bands is seen as the amount of methylated peptide increases.



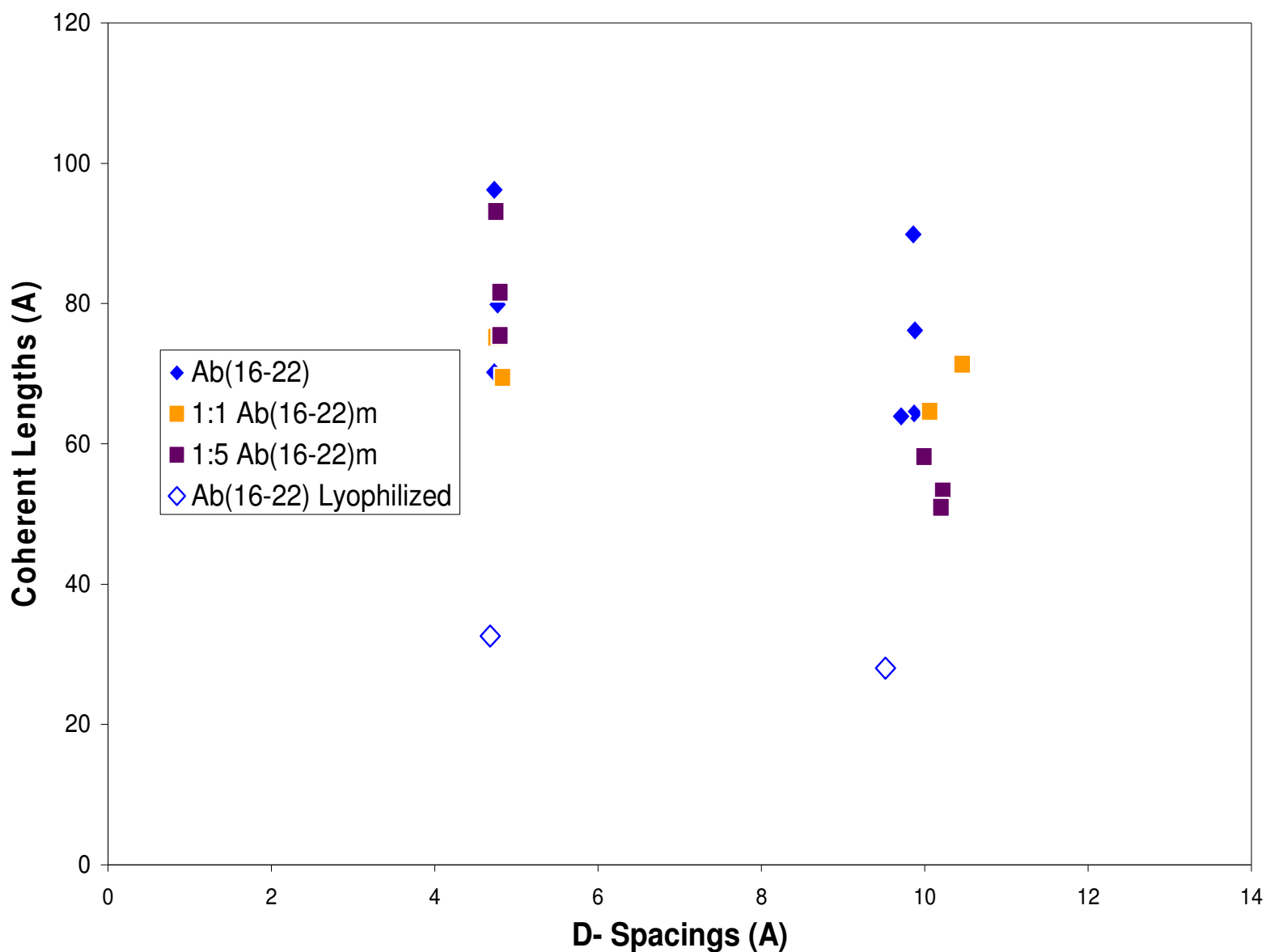
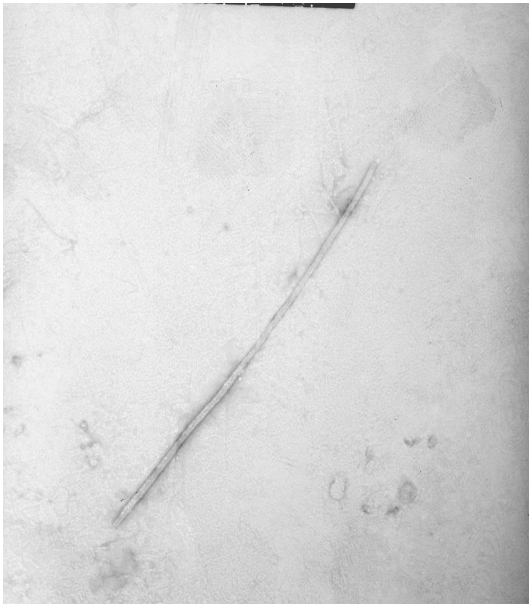


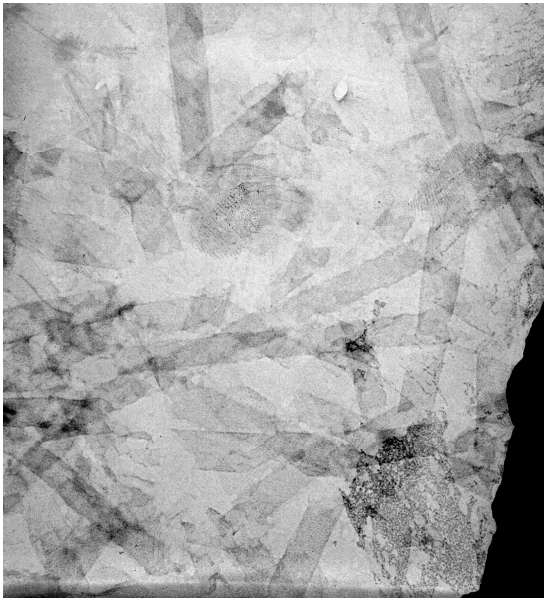
**Figure 2: Analysis of X-Ray Diffraction Patterns for Methylation Study** The points around 4.7 Å represent the hydrogen-bonding direction of fiber formation, and the points around 10.0 Å represent the intersheet stacking direction. While the hydrogen bonding did not differ significantly as the amount of inhibitor increased, the amount of intersheet stacking decreased as the amount of inhibitor increased. The lyophilized peptide is presented as a standard for comparison.



**A.**  $A\beta(16-22)$



**B.** 1:1  $A\beta(16-22)$ :  $A\beta(16-22)m$

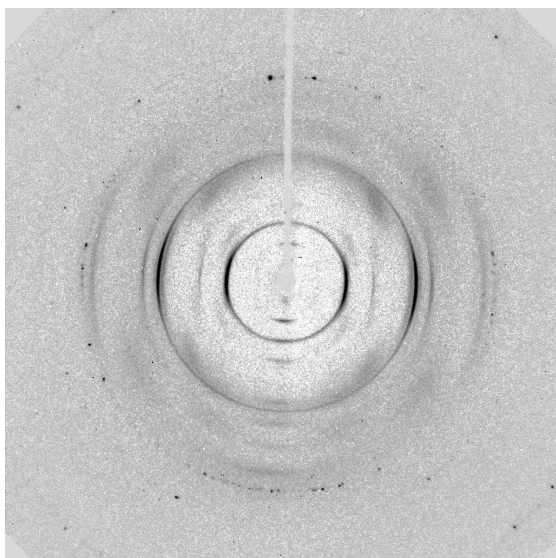


**C.** 1:1  $A\beta(16-22)$ :  $A\beta(16-22)m$

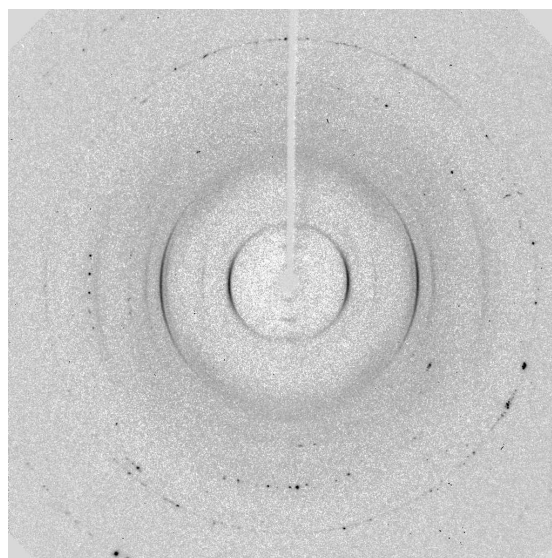


**D.** 1:1  $A\beta(16-22)$ :  $A\beta(16-22)m$

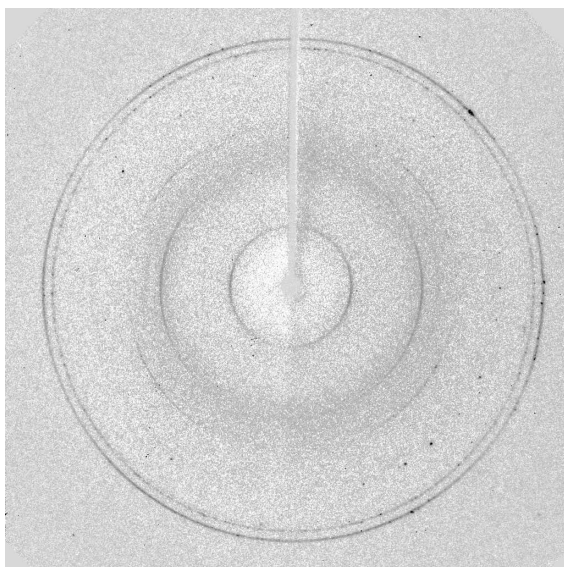
**Figure 3:** TEM micrographs of  $A\beta(16-22)$ . Both figures 2.A and 2.B are taken at 39000x magnification. 2.C is taken at 28500x, and 2.D at 11500. B and C are pictures from the same grid to show the uniform density of the plate-like fibers.



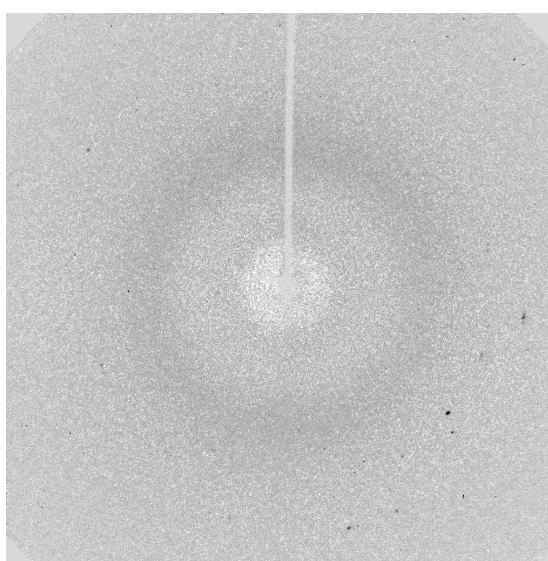
**A.** A $\beta$ (16-22)



**B.** A $\beta$ (16-22) F19CN



**C.** A $\beta$ (16-22) F20CN



**D.** A $\beta$ (16-22) F19/20CN

**Figure 4:** Background-subtracted solubilized/dried XRD patterns of peptides for the cyanophenylalanine study. 20CN has a decrease in both hydrogen bonding and intersheet stacking compared to 19CN, and 19/20CN lacks a significant amount of ordered structure.

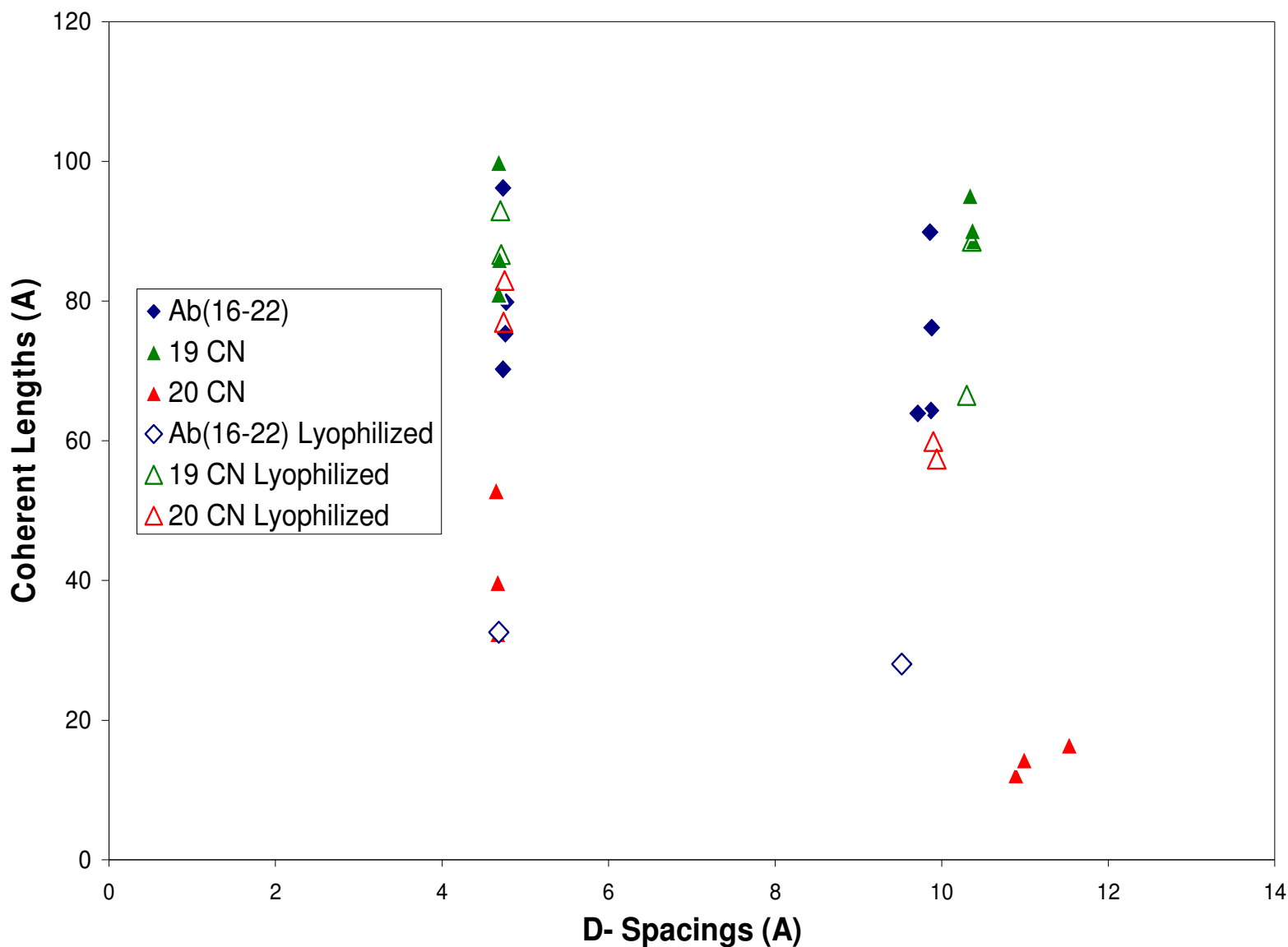


**Figure 5: Analysis of X-Ray Diffraction Patterns for Cyanophenylalanine Study**

The 19 CN samples did not have a significant change in hydrogen bonding, and tended to increase the amount of intersheet stacking as compared to the wild type and its lyophilized form. There was an increase in the distance between sheets though. The 20 CN samples showed decreases in both hydrogen bonding and intersheet stacking, plus a large change in the distance between sheets, as compared to the wild type and its lyophilized form.

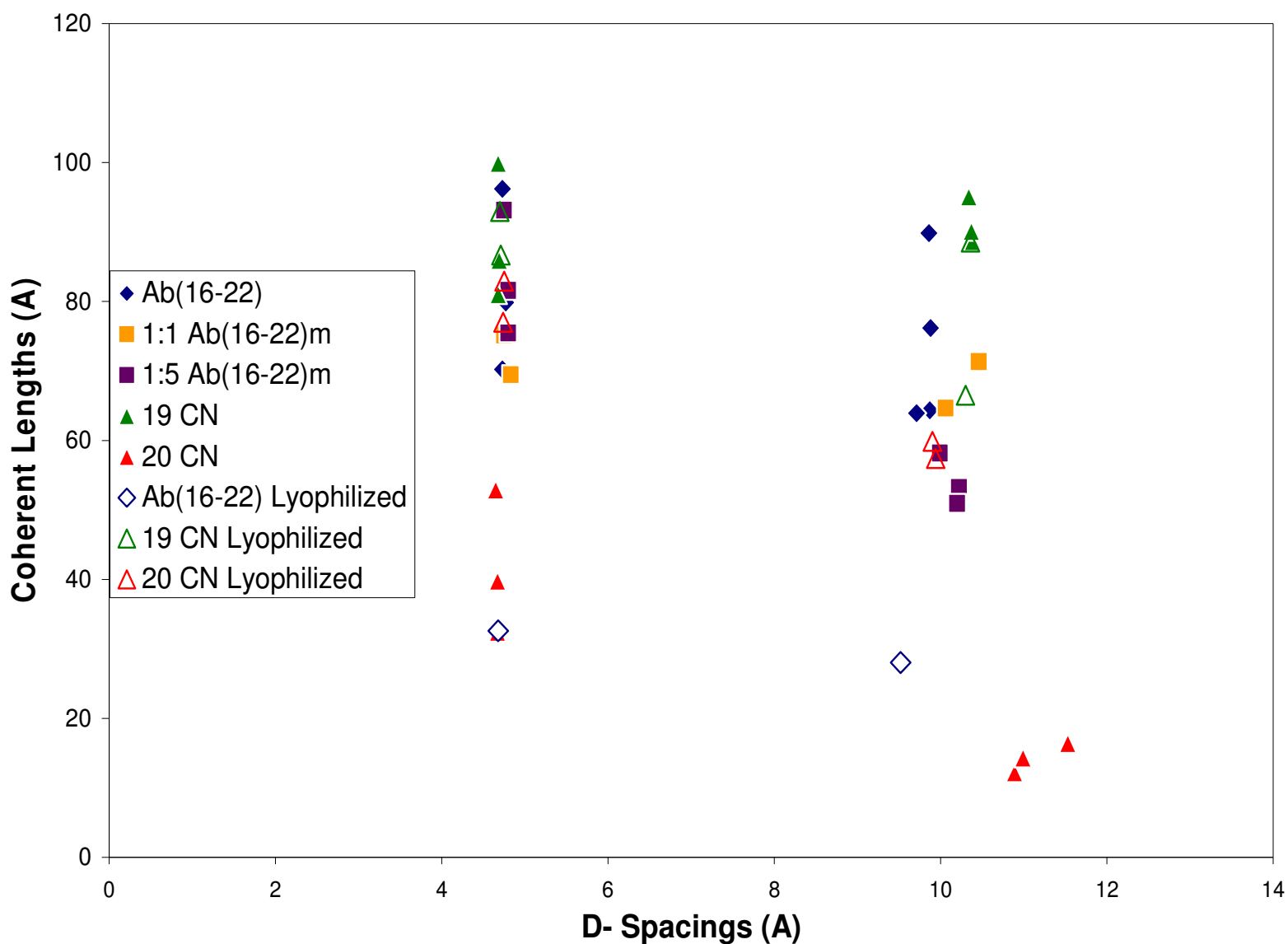


**Figure 6: Combined Data Points from Both X-Ray Diffraction Studies** The methylated peptides are more efficient at limiting intersheet stacking than the 19 CN-substituted peptide. 20 CN is significantly the most efficient, and the only peptide that limits hydrogen bonding.

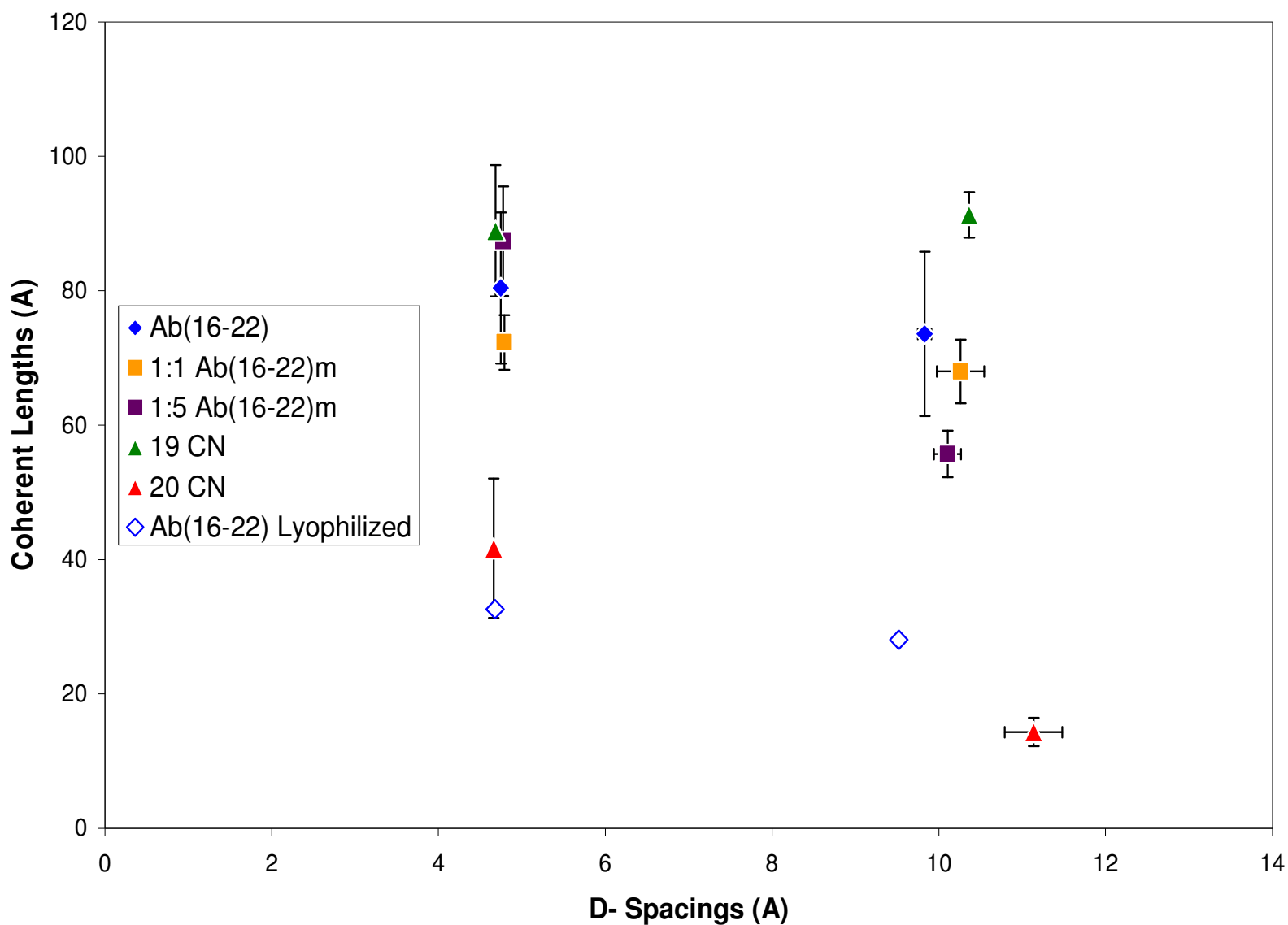


**Figure 7: Combined Data from Both X-Ray Diffraction Studies with Error** The error bars represent the standard deviation from the arithmetic mean of each sample population. This more clearly shows the differences between samples, particularly the coherent lengths of the intersheet stacking direction of the fiber formation.